Reference List

Yamato 980459 – 82.46 grams
Depleted Olivine-phyric Shergottite

Figure 1: *Sawn surfaces of Martian meteorite Y980459 (Misawa 2004). Note the fusion crust and the yellow olivine. See additional photos in Misawa 2004. Cube is 1 cm.*

Introduction

Martian meteorite Y980459 was collected near Minami-Yamato Nunataks by the Japanese field party in 1998 (figure 1). Y980459 was initially announced in Japanese Meteorite Newsletter #11 (2002) and is listed in Meteoritical Bulletin 87, appendix 2 (Russell *et al.* 2003). Y980459 has been the subject of an integrated consortium study (Misawa 2003, 2004).

Y980459 is an olivine shergottite like EETA79001, DaG476 and SaU005, but it appears to have an exposure age more like that of regular shergottites (*see below*). It is very depleted in light rare-earth-elements, has the most magnesian olivine megacrysts of any Martian meteorite and is apparently lacking in plagioclase (Mikouchi et al. 2004; Greshake et al. 2004). The composition of Y980459 has been chosen for high-pressure experiments aimed at determining the mineralogy of the source region (mantle?).

A crystallization age of 472 ± 47 m.y. has been determined, with an exposure age of about 1-2 m.y.

Petrography

Y980459 is a porphyritic basalt with devitrified glassy matrix and no plagioclase (nor masklynite). Yellow olivine phenocrysts are apparent in hand specimen and prominent in thin section (figures 1-3). Y980459 is not only very mafic in composition, but also appears to be very reduced and perhaps "primitive" (McKay et al. 2004). Lentz and McSween (2005) find that the Y980459 magma "*must have begun cooling slowly at depth, while olivine megacrysts grew, but then, - - - a shift in crystallization conditions occurred, probably associated with magma rizing to the surface. Groundmass olivine then began to nucleate and crystallize together*".

Olivine megacrysts (figures 3, 4) contain magmatic melt inclusions which are still glassy (Ikeda 2003, 2004; Mikouchi *et al.* 2004) and chromite grains (Mikouchi *et al.* 2003; Greshake *et al.* 2003). Where olivine, and/or pyroxene phenocrysts are touching, Fe-enrichment of the rims is less pronounced. Olivine megacrysts show patchy undulatory extinction. Ikeda (2003, 2004)

Mineralogical mode of Y980459

	Ikeda 2003, 2004	Greshake *et al.* 2003	Mikouchi *et al.* 2003, 2004	Greshake (CIPW norm) et al. 2004
Olivine	8.7 vol. %	15.7	26	19.4
Plagioclase				12.6
Pyroxene	52.7	52.6	48	63.4
Chromite	0.7	0.5		0.5
Pyrrhotite	0.4	0.3		0.3
Glass	37.4	30.9	25 % mesostasis	
Phosphates				0.5
SiO2 polymorphs				2.7
Melt inclusions		0.1		

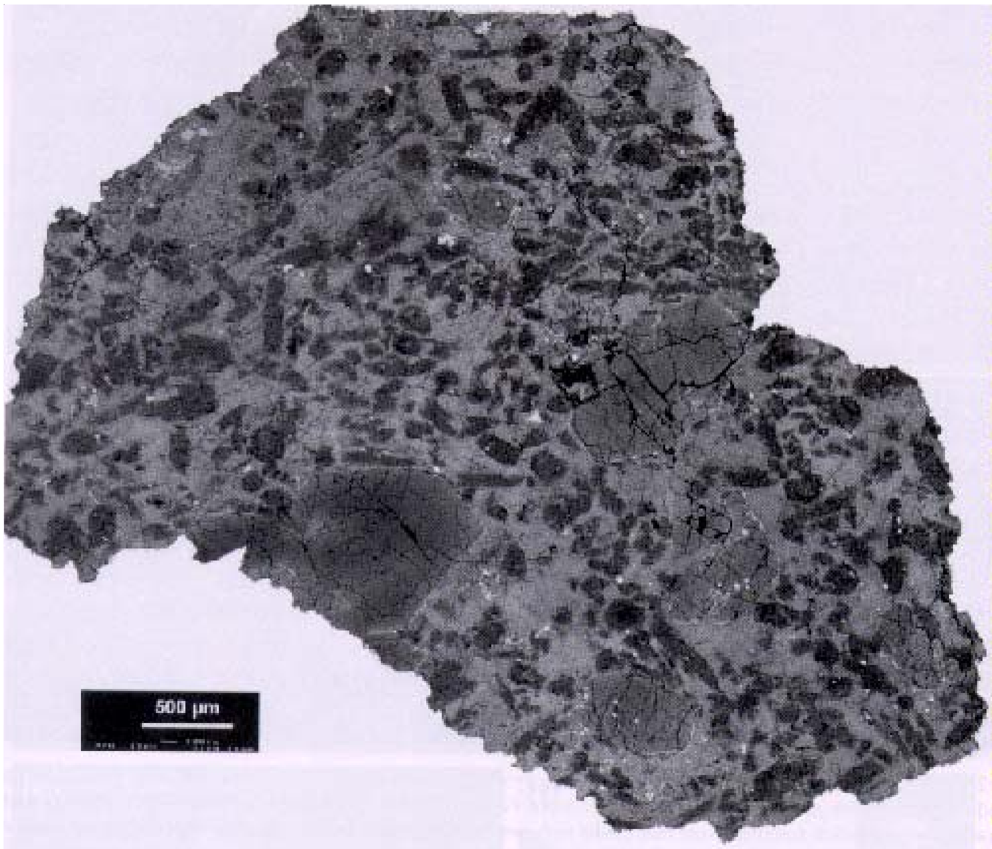

***Figure 2:** Back-scattered-electron (BSE) image of Yamato 980459 showing large olivine megacrysts and smaller pyroxene phenocrysts embedded in fine-grained groundmass (from Greshake et al. 2004).*

and Mikouchi *et al.* (2003, 2004) studied shock-melt pockets. Greshake *et al.* (2003, 2004) estimate peak shock pressure 20-25 GPa.

The mesostasis is dark-colored and glassy (figure 3). It has abundant very-fine-grained dendritic grains of olivine and pyroxene, often in feathery chains (Usii et al. 2009). Some olivine grains in the mesostsis area are present as long blades reaching a few hundreds microns long (Mikouchi *et al.* 2004).

Mineral Chemistry

Olivine: Large olivine crystals (up to 2 mm) are chemically zoned (Fo_{84-33}) and frequently form glomerophyric "clumps" (Greshake et al. 2004; Usii et al. 2009). Koizumi et al. (2004) and Mikouchi et al. (2004) reported olivine cores as Mg-rich as Fo_{86}. Smaller olivine crystals are Fe-rich (Fo_{44}) and feathery olivine dendrites in the quenched residual material are Fo_{29}.

Pyroxenes: The pyroxenes in Y980459 have been analyzed by Koizumi et al. (2004), Mikouchi et al. (2004), Ikeda (2004), Greshake et al. (2004) and Usii et al. (2009). Pyroxene is zoned from an orthopyroxene core ($\sim En_{80}Fs_{18}Wo_2$), to pigeonite ($En_{78}Wo_5$), with finally a thin augite rim ($En_{70}Wo_{35}$) (figure 5). Greshake *et al.* (2003, 2004) find that the Al_2O_3 content of the pyroxene continuously increases out to the rim where it can be as high as 8.5 wt %. Al_2O_3 and TiO_2 are particularly enriched in augite in the mesostasis (Mikouchi *et al.* 2004) apparently due to lack of plagioclase formation.

Plagioclase or Maskelynite: none

Glass: This sample has a glassy residual matrix that is quenched with feathery microlites of sulfide, opaques, olivine and pyroxene (McKay *et al.* 2003; Usii et al. 2009). There is also glass in shock-melt pockets.

Chromite: Chromite in Y980459 is Ti-poor (Ti < 0.4%) (Greshake et al. 2004). Careful analysis of chromite and comparison with chromite formed in reducing conditions, shows that the oxygen fugacity of Y980459 was very low (reduced) (McKay et al. 2004).

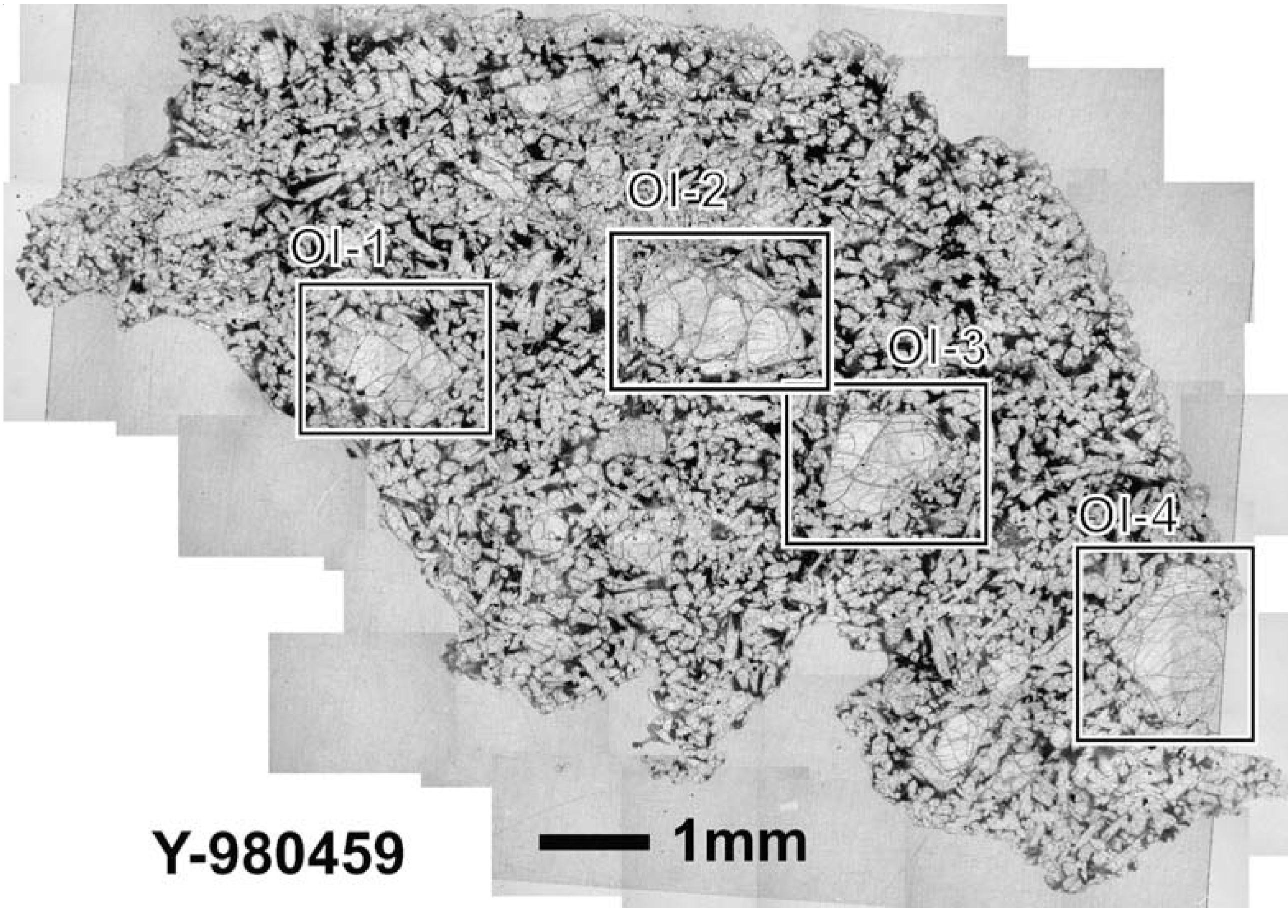

Figure 3: *Transmitted light photomicrograph of Y980459 showing olivine and pyroxene megacrysts in glassy mesostasis (Usii et al. 2008).*

Sulfide: Sulfide is identified as pyrrhotite with up to 2 wt. % Ni.

Phosphate: none

Whole-rock Composition

The chemical composition of Y980459 has been determined by Haramura (reported in Misawa 2003), Dreibus *et al.* (2003) and Shirai and Ebihara (2004) (Table 1). Trace elements have been reported by Shirai and Ebihara (2004) and Nakamura *et al.* (2003) (figure 6). Note that Y980459 is extremely depleted in LREE. Brandon et al. (2012) have determined the PGE and Re (figure 8).

Radiogenic Isotopes

Shih *et al.* (2005) determined a Sm-Nd isochron age of 472 ± 47 Ma (figure 7). A Rb-Sr isochron has proven hard to determine due to lack of plagioclase and the apparent terrestrial alteration or contamination in this rock. *However, Shih et al. (2004) reported a preliminary, contradictory, Rb-Sr age of 296 ± 90 m.y.*

Cosmogenic Isotopes

The cosmic-ray exposure ages calculated from ^{3}He, ^{21}Ne and ^{38}Ar are 1.6, 2.5 and 2.1 m.y., respectively (Nagao and Okazaki 2003 and Okazaki and Nagao 2004). Christen et al. (2004) also found disagreement between these methods and suggest that the average is 2.5 m.y. However, the exposure age determined by ^{10}Be is 1.1 $\pm$ 0.2 m.y. (Nishiizumi and Hillegonds 2004). They suggest that this difference might be attributed to a pre-exposure history (while on Mars ?).

Other Studies

Oxygen isotopes determined by Clayton are ä^{17}O = 2.52 ‰, ä^{18}O = 4.31 ‰; with Ä^{17}O = +0.28 ‰. The activity of ^{26}Al and ^{41}Ca was determined by Nishiizumi and Hillegonds (2004). Okazaki and Nagao (2004) determined the isotopic composition of He, Ne, Ar, Kr and Xe.

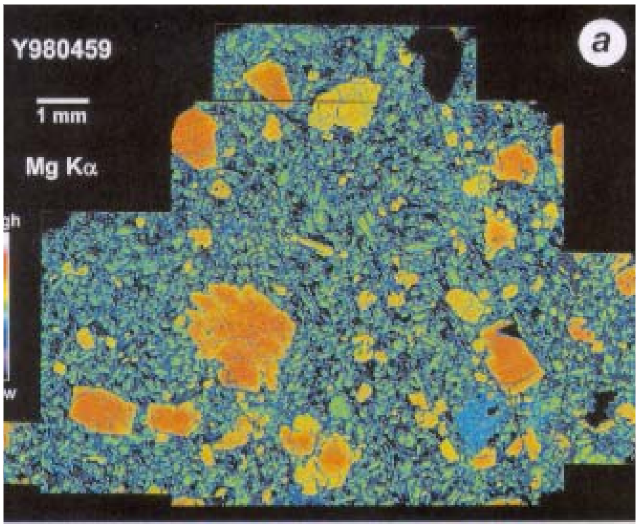

Figure 4: Mg X-ray map of polished section of Y980459 showing mafic olivine megacrysts (orange) (from Mikouchi et al. 2004).

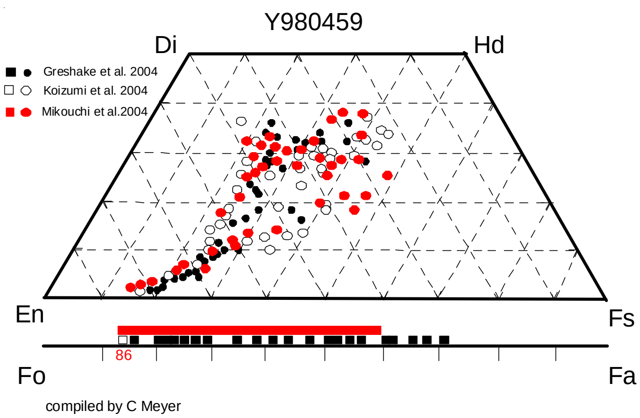

Figure 5: Pyroxene and olivine composition of Y980459 (from Gresheke et al. 2004, Koizumi et al. 2004 and Miyamoto et al. 2004).

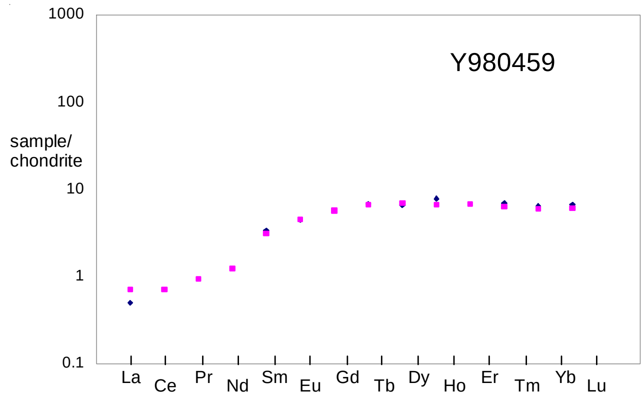

Figure 6: REE diagram for Y980459 (blue from Dreibus et al. (2003), pink from Shirai and Ebihara 2004). Note the extreme depletion in the light REE.

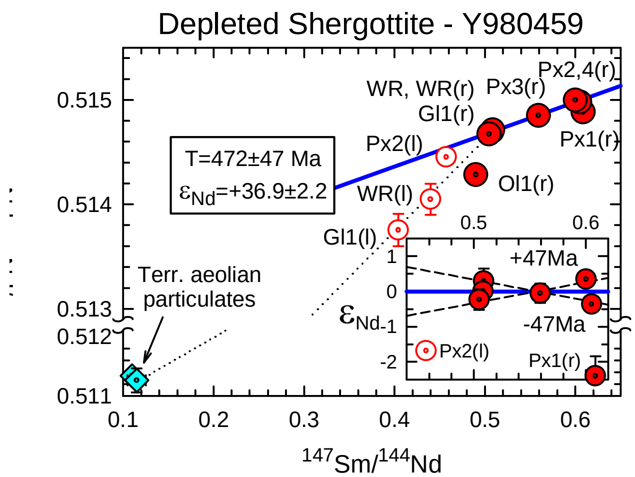

Figure 7: Sm-Nd isochron for Y980459 (from Shih et al. 2005).

Norris and Herd (2006) and Draper (2009) have used the rather mafic composition of Y980459 for experiments to determine the phase relationships in the Martian mantle at pressures in the range of 10-20 kilobars. Shearer et al. (2006) are trying to used vanadium portioning to determine the oxygen fugacity, while Symes et al. (2006) are trying to "model" the trace element behavior during fractional crystallization.

Hiroi et al. (2005) have determined the visible and IR spectra.

Processing

The processing and distribution of Y980459 is described in Misawa (2003 and 2004). The figures in these reports indicate two (2) saw cuts. A summary "consortium report" is expected. See http://yamato.nipr.ac.jp/AMRC/amr17/AMR1701.pdf

References for Y980459

Table 1. Chemical composition of Y980459.

reference	Haramura (d)		Dreibus 03		Shirai 04		Greshake 04		Nakamura 03
weight	1.4 g				2.585 g				see dia.
SiO2	48.7	(a)			49.9		49.4	(c)	
TiO2	0.54	(a)			0.532		0.48		
Al2O3	5.27	(a)			5.17		6		
FeO *	17.53	(a)	18.24	(b)	17.3	(b)	15.8		
MnO	0.52	(a)	0.49	(b)	0.481	(b)	0.43		
CaO	6.37	(a)	5.88	(b)	6.83	(b)	7.2		
MgO	19.64	(a)			18.7		18.1		
Na2O	0.48	(a)	0.68	(b)	0.651	(b)	0.8		
K2O	<0.02	(a)			0.0156	(b)	0.02		
P2O5	0.29	(a)					0.31		
sum									
Li ppm			1.3	(b)					
F			86	(b)					
Cl			57	(b)	64.4	(b)			
Sc			36.4	(b)	34.9	(b)			
V					188	(b)			
Cr	4858	(a)			4755	(b)			
Co	70	(a)	56.2	(b)	51.6	(b)			
Ni	270	(a)	240	(b)	203	(b)			
Cu									
Zn			76	(b)	81.1	(b)			
Ga			11	(b)					
Ge									
As			<0.2	(b)					
Se			<0.9	(b)					
Br			0.205	(b)					
Rb									
Sr									
Y									
Zr									
Nb									
Mo									
Pd ppb									
Ag ppb									
Cd ppb									
In ppb									
Sb ppb									
Te ppb									
I ppm									
Cs ppm									
Ba			<30	(b)	1.54	(d)			
La			0.12	(b)	0.166	(d)			
Ce			<0.7	(b)	0.426	(d)			
Pr					0.0841	(d)			
Nd					0.567	(d)			
Sm			0.498	(b)	0.466	(d)			
Eu			0.25	(b)	0.254	(d)			
Gd					1.13	(d)			
Tb			0.25	(b)	0.244	(d)			
Dy			1.6	(b)	1.7	(d)			
Ho			0.44	(b)	0.379	(d)			
Er					1.09	(d)			
Tm			0.17	(b)	0.155	(d)			
Yb			1.05	(b)	0.971	(d)			
Lu			0.164	(b)	0.15	(d)			
Hf			0.49	(b)					
Ta									
W ppb									
Re ppb									
Os ppb									
Ir ppb			<5	(b)					
Au ppm			1.5	(b)					
Tl ppb									
Bi ppb									
Th ppm			<0.1	(b)	0.0213	(d)			
U ppm			<0.02	(b)	0.006	(d)			

technique: (a) wet, (b) INAA, (c) Mode and elec. Probe, (d) ICP-MS * recalculated

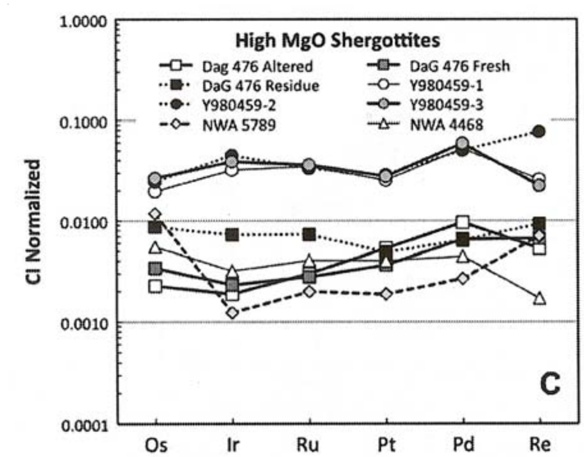

Figure 8: *PGE and Re from Brandon et al. 2012.*